Susceptibility Corrected Myocardial R2* Quantification with Magnetic Resonance Imaging

Shane A Wells[1], Karl K Vigen[1], Jeffrey S Nackos[1], Scott B Reeder[1,2], and Diego Hernando[1]

[1]*Department of Radiology, University of Wisconsin-Madison, Madison, WI, United States,* [2]*Department of Medical Physics, University of Wisconsin-Madison, Madison, WI, United States*

Introduction: Excess myocardial iron can result in sudden death or heart failure, the leading causes of morbidity and mortality in patients receiving chronic blood transfusions [1]. Quantitative assessment of myocardial iron is needed for diagnosis, staging and treatment monitoring of cardiac iron overload. R2*-MRI, based on quantifying R2* relaxivity from a sequence of gradient echo images with increasing echo times, is an effective technique to assess myocardial iron [2]. Unfortunately, R2* is affected by confounding factors, particularly undesired susceptibility effects [3]. Susceptibility effects are severe near tissue/air interfaces (eg: heart/lung interface) and result in Bo field variations and rapid signal dephasing [4]. This dephasing introduces errors in R2* measurements, and these errors are heavily dependent on protocol (e.g., slice orientation and thickness). Recently, a method was introduced to perform susceptibility-corrected R2* mapping [5]. Susceptibility correction is performed by measuring the Bo field from the acquired complex data then correcting for the effect of field variations within each voxel. In this work, we evaluate the susceptibility correction for cardiac R2* mapping in a cohort of 10 healthy subjects without iron overload.

Materials and Methods: The study was approved by our institutional review board and was HIPPA compliant. After obtaining informed written consent, 10 healthy volunteers (10 men, mean age 35.6 years, range 25-43) were prospectively imaged at 1.5 T (Signa HDxt Echospeed, GE Healthcare, Waukesha, WI) using an eight-channel phased array cardiac coil during breath holding (single breath-hold per slice). Prospective ECG-gated cardiac imaging was performed with 2D multi-echo SPGR [6], with parameters: LV short-axis view, FOV=35x28cm, Matrix=192x154, 12-14 slices, Thickness/Spacing=8mm/0, TR/TE_1/ΔTE/RBW=19.5ms/2.1ms/2.0-2.2ms/±83.3kHz, FA=20°, 8 echoes/TR, 2xRR, 12-16 views per segment (depending on heart rate). Reconstruction consisted of two key steps: 1) fat and water images, Bo field map and uncorrected R2* map were estimated using a standard fat-water separation algorithm [7]; 2) the gradient of the measured Bo field was calculated to determine the additional signal decay introduced at each voxel (accounting for slice profile via Bloch equation simulation), which was then included in the signal model to produce susceptibility-corrected R2* [5]. Uncorrected R2* and corrected R2* were measured by placing a region-of-interest (ROI) [mean 68mm^3, range 57-78mm^3] in each AHA cardiac segment, except the apical segment (#17, not consistently visualized on the short-axis and therefore not included). Each cardiac segment ROI (Advantage Workstation, GE Healthcare, Waukesha, WI) was placed on the water image which served as an anatomical localizer for each AHA segment, then copied to the uncorrected and corrected R2* maps, to achieve precise co-localization. Mean and standard deviation of uncorrected and corrected R2* was calculated for each cardiac segment.

Results: Figure 1 illustrates an example of apparent increased myocardial R2* in the inferolateral wall (segment 11) at the myocardial-air interface on the uncorrected R2* map that improves dramatically with susceptibility correction. Figure 2 summarizes the results for the cardiac segments in all ten subjects, demonstrating wide variations in apparent myocardial R2* across segments, and among subjects (large standard deviations). This was most noticeable in segments located near myocardial-air interfaces (segment 10-12, 14 and 16) on the uncorrected R2* maps. Unexpectedly, the largest variation in apparent R2* occurred in the septum (segment 3) previously thought to be relatively free of susceptibility artifact. Susceptibility correction substantially improved the apparent wide variations in myocardial R2* seen in uncorrected R2*, with greatly reduced variation across segments.

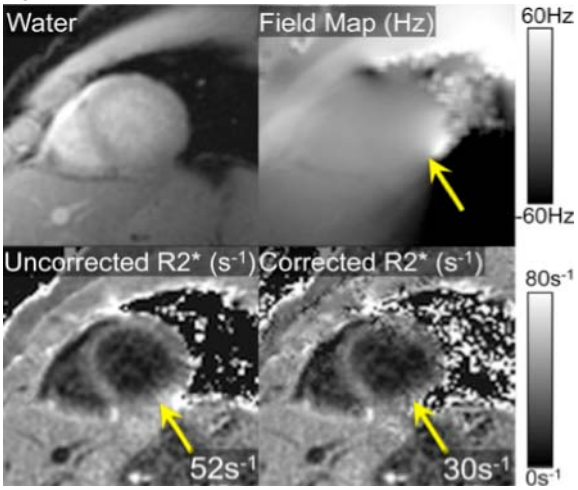

Figure 1: Susceptibility-correction removes focal increases in apparent R2* (arrow) caused by focal Bo field inhomogeneities.

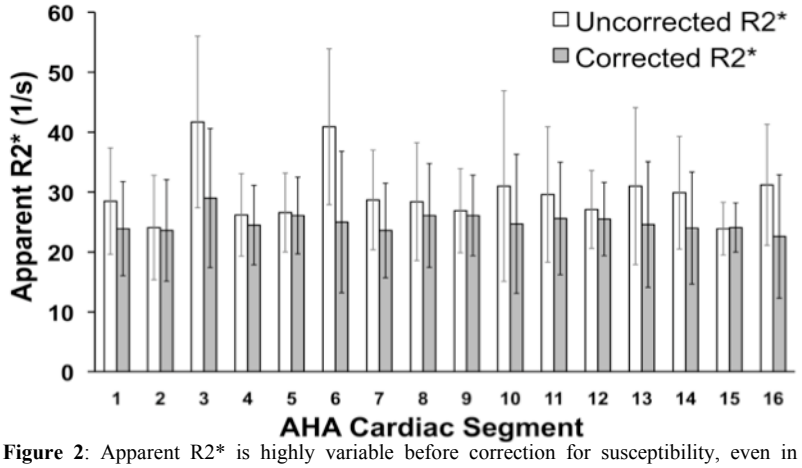

Figure 2: Apparent R2* is highly variable before correction for susceptibility, even in normal subjects (N=10). After susceptibility correction,measured R2* values were more consistent across cardiac segments. The apical segment (AHA #17) was not consistently visualized on short axis imaging and therefore not included in these measurements.

Discussion: Accurate, reproducible, noninvasive quantification of myocardial iron is important as it provides both prognostic and therapeutic clinical information. While the cardiac septum has been previously demonstrated to suffer little from B_0 inhomogeneity, apparently inhomogenous myocardial iron measurements due to undesired susceptibility effects can result in spurious results and possibly deleterious treatment-related consequences. Furthermore, susceptibility artifact within the cardiac septum can also occur, as demonstrated here, thus potentially resulting in falsely elevated R2* with conventional methods. Here we have demonstrated the feasibility of an R2* map susceptibility correction technique.

Conclusion: R2* measurements in the heart demonstrate greatly increased consistency and less variability if susceptibility correction is used. Future work will investigate the utility and need for susceptibility correction in patients with known or suspected cardiac iron overload.

References: [1] Olivieri NF et al, NEJM 1994;331:574–8. [2] Di Tucci AA et al, Haematologica 2008;93:1385-8. [3] Fernandez-Seara et al MRM 2000;44:358-66. [4] Reeder SB et al, MRM 1998;39:988-98. [5] Hernando D et al, MRM 2011 (In press). [6] Vigen KK et al, ISMRM 2009, #2775. [7] Yu H et al, MRM 2008;60:1122–34.

Acknowledgements: We acknowledge the support of the NIH (R01 DK083380, R01 DK088925 and RC1 EB010384), the Coulter Foundation, WARF Accelerator Program and GE Healthcare.